Energy and Buildings 139 (2017) 578–589

Contents lists available at ScienceDirect

Energy and Buildings

journal homepage: www.elsevier.com/locate/enbuild

Parametric modelling of domestic air-source heat pumps

C.P. Underwood [a,*], M. Royapoor [b], B. Sturm [c]

[a] Faculty of Engineering and Environment, University of Northumbria, UK
[b] Sir Joseph Swan Centre for Energy Research, Newcastle University, UK
[c] Postharvest Technologies and Processing Group, Kassel University, Germany

ARTICLE INFO

Article history:
Received 25 August 2016
Received in revised form 6 January 2017
Accepted 9 January 2017
Available online 12 January 2017

Keywords:
Air-source heat pump
Heat pump modelling
Compressor modelling
Defrosting
Performance gap

ABSTRACT

A new domestic air-source heat pump model is proposed which can be parameterised either from field data, experimental data or manufacturers' standard rating data. The model differs from the much more prevalent system-side regression models for these types of heat pumps in that it operates on refrigerant-side variables. This makes it more suited to detailed performance analyses of heat pumps in service. Because both field data and manufacturers' data can be used for parameterising the model, it can be used to investigate problems associated with the building performance gap where a heat pump is used. A new type of efficiency-based compressor model is developed which enables compressor performance to be directly compared with alternatives and a model of defrosting is included by introducing a new defrost discounting term. Results tested using data from a field monitoring site and from a laboratory installation show good predictive behaviour by the model especially at low source air temperatures. When the model is fitted using manufacturer's standard rating data, a performance gap is evident when compared with the model fitted to field data but the gap is generally nominal.

1. Introduction

Most domestic air-source heat pumps in Europe sink to hot water heating systems and generally consist of second-generation technologies. Typically, this is characterised by the use of a hydro-fluoro-carbon working fluid, scroll compressors, compact brazed-plate condensers, mechanical expansion device and conventional fin and coil evaporators. Controls usually consist of fixed speed thermostatic control over the compressor and defrosting is effected through the use of reverse-cycling changeover controls. These heat pumps are becoming well established in Europe and north America and are expected to enjoy increased use in other countries in the coming years. In the UK for example, a sharp increase in their use is envisaged for domestic space heating in the coming years in order to address the twin aims of reducing carbon emissions as well as to diversify away from an over-dependence on gas for space heating [1].

Recent field trials of domestic air-source heat pumps in the UK have revealed seasonal performance factors of the order of 2.5 [2,3]. Gleeson and Lowe conducted a detailed comparison of UK and European field trials for domestic heat pumps which concluded that UK performances are generally inferior to those observed in other European countries [4]. The reasons mentioned for better European performances include minimal use of back-up heating; the use of compensating heating control; higher quality heating systems in terms of components and controls; a low usage of domestic hot water (at higher temperatures) and higher house insulation standards. Hence there is a significant 'performance gap' [5] concerning UK heat pumps in service.

There is a need for a better understanding of how these systems perform in practice when matched to alternative house construction, heating system design, hot water usage, system control and operation, and user behaviour. To assist with this requires better modelling of the performance of these heat pumps in service as informed by the new field trial data that is beginning to become available [2,3]. Historically, deterministic models of heat pump behaviour have been developed but these require a high level of detailed information about the heat pump and its control to make them feasible. Many existing heat pumps systems can be categorised as 'information poor' in which certain key data are either unavailable due to commercial sensitivity or are uncertain. This has led to 'black box' modelling or boundary variable modelling in which heat pump behaviour is fitted to field observations of ambient air temperature and, optionally, heating system temperature. These approaches require much less information but result in a lack of predictive detail that might otherwise be used to help diagnose

* Corresponding author.
E-mail address: chris.underwood@northumbria.ac.uk (C.P. Underwood).

http://dx.doi.org/10.1016/j.enbuild.2017.01.026
0378-7788/

List of symbols

$a...f$	Model-fitting parameters
CoP	Coefficient of performance
f(...)	(a function of)
F_{df}	Defrost discount factor
H_{ero}	Refrigerant enthalpy at evaporator outlet ($kJkg^{-1}$)
H_{cri}	Refrigerant enthalpy at compressor outlet ($kJkg^{-1}$)
H_{cro}	Refrigerant enthalpy at condenser outlet ($kJkg^{-1}$)
m_r	Refrigerant mass flow rate (kgs^{-1})
P_e	Evaporating pressure (kNm^{-2})
P_c	Condensing pressure (kNm^{-2})
Q_c	Average (steady) condenser heat output (kW)
$Q_{c,df}$	Defrost-adjusted average condenser heat output (kW)
R_p	Compression ratio ($=P_c/P_e$)
$SCoP$	Seasonal coefficient of performance
SPF	Seasonal performance factor
SPF_{H2}	Seasonal performance factor including heat pump auxillary loads
T_{ao}	External air temperature (°C)
T_e	Evaporating temperature (°C)
T_c	Condensing temperature (°C)
T_{cwo}	Condenser water outlet temperature (°C)
V_d	Compressor displacement volume (m^3s^{-1})
W	Average (steady) overall compressor plus auxillary power (kW)
W_{aux}	Auxillary power (kW)
W_i	Average compressor isentropic work (kW)
Greek:	
ΔT_c	Condenser thermal approach (K)
ΔT_e	Evaporator thermal approach (K)
η_i	Compressor isentropic efficiency
η_v	Compressor volumetric efficiency
γ	Compression index of an ideal gas
ρ_{suc}	Refrigerant density at compressor inlet (kgm^{-3})
Vectors:	
C	1×2 cost function of RMSE values
Goal	1×2 vector of target optimisation goals
I	1×2 vector of inputs
O	1×2 vector of outputs
P	1×10 vector of model fitting parameters
$\mathbf{P}^-$	1×10 vector of model fitting parameter lower bounds
$\mathbf{P}^+$	1×10 vector of model fitting parameter upper bounds

the extent of under-performance and what might be done about it. (For a general review of approaches to modelling heat pump systems generally, see [6].) This work attempts to address these limitations by developing a new type of heat pump model that can be readily fitted to field monitoring data or manufacturers standard rating data so that heat pump performance revealing performance gaps and other departures from expected operational behaviour can be identified.

In this work a new model is developed that can be readily fitted to average performance data and/or data arising from standard rating information. At the heart of this model is a new compressor model which can be fitted with a relatively small number of parameters and is able to capture the (varying) compressor isentropic efficiency. Because the model can be fitted to field data as well as standard rating data, it is possible to compare expected heat pump performance with actual heat pump performance in the field. The objectives of this work are summarised as follows:

- To develop a domestic air-source heat pump model that can be fitted to a variety of data sources with sufficient detail to enable both heat pump and compressor performance in service to be determined
- To student defrost activity of heat pumps in service and incorporate adjustments to the model to take account of defrosting
- To test the model against field monitoring and laboratory data
- To compare a model fitted to field monitoring data with a model fitted to standard rating data in order to quantify the heat pump performance gap
- To compare the results of the two alternative models with recent results reported from extensive field monitoring

2. Review

Numerous attempts have been made to fit simple regression models to heat pump field data based on boundary variables only [7–10]. Gupta and Irving [7] describe the development of a regression model giving seasonal performance factor (*SPF*) as a function of temperature lift (heating 'sink' temperature minus source temperature) for a variety of source types including air. However the model is based on field results observed in Switzerland which, as Gleeson and Lowe have noted [5], have exhibited higher performances than in the UK which raises issues about the robustness of this model when used in UK applications. Also, it is not clear as to whether and how defrosting has been accounted for in the air-source heat pumps. Murphy et al. [8] develop a 5-parameter regression model of an air-source heat pump with ambient air temperature and heating system return water temperature as independent variables. The model is incorporated in a general building thermal model and results are found to be within field trial data. Tabatabaei et al. [9] compare the accuracy of first, second, third and fourth-order polynomial models of air-source heat pump *SPF* with just external air temperature as the independent variable by fitting to field monitoring data from a number of sites in Belgium. They conclude that best results arise from the higher-order models. Touchie and Pressnail [10] fit simple linear models to experimental data to predict the *CoP* versus external air temperature and compare the results with manufacturer's data. (The experimental test set up used a warm buffer zone to mitigate the effects of very cold source air in extreme winter conditions.) Results show that the test data *CoP* values vary with the same slope as the manufacturer's data but the *CoP* values themselves are much lower for a number of reasons.

In one of few models explicitly considering part-load performance, Madonna and Bazzocchi [11] develop a simple model of reversible air-to-water heat pumps by using field data to derive adjustments to a maximum coefficient of performance value which is based on a modified Carnot performance. Further fitted terms allow for part-load and defrost operation. The model is integrated with a building simulation tool and applied to buildings in 3 contrasting Italian cities.

In a more detailed parametric approach, Jin and Spitler [12] describe detailed parameter-extraction from manufacturers' catalogue data for water-to-water heat pumps using scroll compressors. The model leads to detailed performance data but is dependent on manufacturers data which itself is usually generated by a model (i.e. their results are not verified against field or laboratory data).

Guo et al. [13] use grey system theory to model air-source water heating systems. This method is suited to time series observations with uncertainty and involves smoothing the data to reduce randomness and then fitting a differential equation based 'grey model'

to the smoothed data. Reasonably representative models can be obtained from situations where data are limited in quantity, incomplete or uncertain but they lack insightful data about detailed plant performance.

Kinab et al. [14] develop a very detailed steady-state model of a reversible air-to-water heat pump which explicitly calculates the compressor efficiency and so can be used to compare compressor performances. However the compressor regression model is parameterised through 18 fitted coefficients (9 each for power and mass flow rate). Results with experimental data for an R410A heat pump are good and a detailed consideration is given to the treatment of defrosting in the model. In one of few detailed studies on defrosting of air-source heat pumps, Qu et al. [15] report on experimental studies carried out on a 6.5 kW heat pump with multiple circuits. Results show the transients in key variables during defrosting and conclude that defrosting is completed more quickly in up-steam circuits than in down-stream circuits. In a follow-on article [16] a detailed semi-empirical model of defrosting is developed which confirms that the protracted down-stream circuit defrosting behaviour is attributed to delays caused by flowing water from melted ice coming from upstream circuits.

In relation to dynamic modelling of air-source heat pumps, Ji et al. [17] develop a dynamic model of a multi-functional heat pump which includes regression-fit models for both refrigerant flow rate and power consumption fitted to manufacturer's data. The fitted equations each involve 6 coefficients (12 in all). Kelly and Cockcroft [18] develop a second-order dynamic model with parameters fitted from experimental data for domestic air-source heat pumps and then used to compare with results from field monitoring. Results are good at low ambient air temperatures but the model tended to over-predict performance at higher temperatures though this was brought into good alignment when temperature compensation was disabled which helped to reveal inappropriate operation in the field.

In summary, though significant progress has been made in relation to air-source heat pump modelling informed by field monitoring data, the resulting models are either too simplistic and cannot be used for detailed equipment performance evaluation, or are too complex and require extensive detailed information for their derivation. What is needed is a model of intermediate complexity which can be fitted reliably from limited data. This is addressed in the work reported here.

3. Parametric modelling

The key component behaviour to capture in a compression-cycle heat pump is that of the compressor. Performances of scroll compressors expressed in terms of isentropic efficiency, η_i, versus compression ratio, R_p, are shown in Fig. 1 for 3 alternative compressor manufacturers (denoted here as 'A', 'B' and 'C' to retain commercial anonymity), two alternative working fluids (zeotrope R407C and near-azeotrope R410A) and condensing temperatures of 50–55 °C. The characteristics show a rise component and a decay component separated by a peak efficiency which occurs at low compression ratio. Exponential growth and decay functions are found to describe this behaviour very well indeed with just 4 parameters. The resulting model is given by Eq. (1) in which $a...d$ form fitting parameters:

$$\eta_i = \frac{a\exp\left(-b\left(R_p - c\right)\right)}{1+\exp\left(-d\left(R_p - c\right)\right)} \tag{1}$$

Results of the fitted models are superimposed as solid lines in Fig. 1 (the manufacturers' data points are shown as crosses). An excellent fit is achieved with a goodness of fit statistic of nearly 1 in all cases. This model has the advantages of requiring far fewer fitting coefficients than other models reported in the literature (i.e. [14,17]), as well as leading to a definitive compressor performance variable – the isentropic efficiency – which can be directly compared with alternative compressor types.

The efficiency can be used in conjunction with the classical analytical model of a compressor, Eq. (2):

$$W_i = \frac{m_r \gamma P_e}{\rho_{suc}(\gamma - 1)}\left(\left(\frac{P_c}{P_e}\right)^{\frac{\gamma-1}{\gamma}} - 1\right) \tag{2}$$

The mass flow rate delivered by the compressor is obtained from the volumetric efficiency, Eq. (3):

$$\eta_v = \frac{m_r}{\rho_{suc} V_d} \tag{3}$$

A reasonable assumption for the variation in volumetric efficiency is a linear function of compression ratio, Eq. (4), [19]:

$$\eta_v = e - fR_p \tag{4}$$

(in which e and f are fitting coefficients).

The overall heat pump electrical power is then obtained from Eq. (5):

$$W = \frac{W_i}{\eta_i} + W_{aux} \tag{5}$$

W_{aux} in Eq. (5) is the auxillary power consumed by the heat pump and is assumed to be constant. For an air-source heat pump this will mainly consist of the power drawn by the source air fan but will also include minor electrical losses associated with the power connections, wiring loom and control circuits.

Note that at: $\frac{d\eta_i}{dR_p} = 0$, the compression ratio at the peak isentropic efficiency can be located. It is possible to show that this can be expressed by Eq. (6):

$$R_p|_{\max(\eta_i)} = \frac{1}{d}\left(cd - \ln\left(\frac{ab}{ad-ab}\right)\right) \tag{6}$$

Therefore the maximum isentropic efficiency can be obtained by applying the value for R_p from Eq. (6) in Eq. (1).

The electrical load consumed by the heat pump can be fully described by 8 model parameters: $a...f$, V_d and W_{aux}. Note that V_d is the leading parameter for heat pump capacity.

The evaporating and condensing temperatures are obtained with reference to a heat exchange thermal approach or 'pinch'. In its simplest terms, the pinch point of a heat exchanger is the difference in temperature between the hot fluid and cold fluid where it is a minimum (i.e. usually at an inlet/discharge connection). For the condenser this will be the difference in temperature between the condensing temperature and the water outlet temperature (i.e. the heating water flow to the heating system which will usually be specified as the controlled heating temperature value). For the evaporator this will be the difference between the source air outlet temperature and the evaporating temperature but, for convenience in the present work, the difference between the source air inlet temperature (the ambient air temperature) and the evaporating temperature will be used. Thus the evaporator pinch will include the temperature drop experienced by the air (typically 3–5 K for domestic heat pumps). These pinch temperature differentials form two further model parameters, ΔT_c and ΔT_e which are used to obtain the evaporating and condensing temperatures as follows:

$$T_c = T_{cwo} + \Delta T_c \tag{7}$$

$$T_e = T_{ao} - \Delta T_e \tag{8}$$

Note that, in this work, refrigerant pressure losses, evaporator superheating and condenser sub-cooling are neglected. It would be an easy matter to include these extra variables but they would each

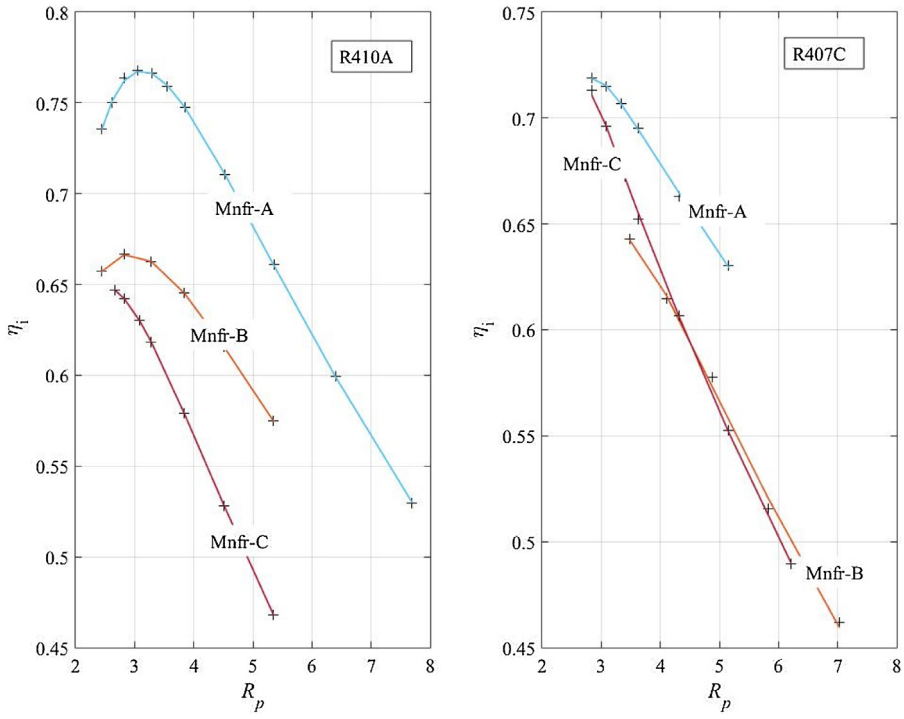

Fig. 1. Efficiency performances of 3 alternative scroll compressors. (Legend: solid lines – fitted models, crosses – manufacturers' data points)

involve one further fitting parameter for what would likely be only a small improvement in model accuracy.

The condensing and evaporating pressures may now be obtained from refrigerant properties:

$$P_{c,e} = f(T_{c,e}) \tag{9}$$

Remaining properties including the refrigerant enthalpy at condenser outlet (hence evaporator inlet), the refrigerant enthalpy at evaporator outlet and the refrigerant suction gas density are similarly obtained from refrigerant properties:

$$H_{cro,ero} = f(P_{c,e}) \tag{10}$$

$$\rho_{suc} = f(P_e) \tag{11}$$

The enthalpy at compressor discharge (i.e. condenser inlet) is now obtained from Eq. (12):

$$H_{cri} = H_{ero} + \frac{W - W_{aux}}{m_r} \tag{12}$$

The refrigerant properties were obtained using NIST REFPROP 8 [20] by direct interpolation as described in [21]. The target heat pump heat output (condenser load) can now be found:

$$Q_c = m_r (H_{rci} - H_{rco}) \tag{13}$$

Finally, the performance of the heat pump for a defined set of boundary conditions is the coefficient of performance, *CoP*. For performance over the extended time horizon of a heating season, the seasonal coefficient of performance, *SCoP*, is applicable and the corresponding seasonal performance based on observations from field or test data is the seasonal performance factor, *SPF*. In this work, only the essential auxillary power usages are included in these performance metrics (i.e. the source air fan and power lost in wiring and control circuits within the heat pump itself). The heating water pump and any top-up heating are excluded. This means that the results presented here refer to the heat pump only. The seasonal performance factor so-defined is sometimes referred to as SPF_{H2} (further details of the various definitions and performance boundaries for heat pumps can be found, for example, in [4]). The coefficient of performance and seasonal coefficient of performance are defined as follows (Eqs. (14) and (15)):

$$CoP = \frac{Q_c}{W} \tag{14}$$

$$SCoP = \int_{Season} Q_c \div \int_{Season} W \tag{15}$$

4. Model fitting

From the previous Section, a heat pump model can be defined from two inputs, **I**. Ten model fitting parameters, **P**, require to be found, and there are two target outputs variables, **O**.

Specifically:

$$\mathbf{I} = \begin{bmatrix} T_{ao} & T_{cwo} \end{bmatrix} \tag{16}$$

$$\mathbf{P} = \begin{bmatrix} a & b & c & d & e & f & V_d & W_{aux} & \Delta T_c & \Delta T_e \end{bmatrix} \tag{17}$$

$$\mathbf{O} = \begin{bmatrix} Q_c & W \end{bmatrix} \tag{18}$$

Model fitting was initially carried out using two data sets: a field monitoring set and a laboratory data set. This would then enable comparisons to be made regarding a heat pump in-service with 'real-world' social user interventions and a heat pump operating under defined conditions free from social interaction.

The field monitoring data set was obtained from an air-source heat pump installation in a 1970s mid-terrace house in Leeds, UK. The house is occupied by a family of 5 and has 3 bed rooms and has been upgraded with cavity wall insulation, roof insulation, double-glazed (UPVC) windows. New heating radiators were installed with the heat pump and sized to operate at lower circulating temperatures (45 °C). The heat pump also connects to a baseload coil in a hot water tank (which has a top-up electric immersion heater).

The laboratory air-source heat pump is also of domestic-scale and though larger, has many technical details in common with the field installation. It is connected to 4 low-grade heating radiators (sized to operate nominally at 40 °C) which are used to heat the local laboratory environment.

Table 1
Details of the test heat pumps.

Description	Field installation	Laboratory installation
Rated heat[a] (A7-W35)	5.92 kW	10.2 kW
Rated power[a] (A7-W35)	1.64 kW	2.83 kW
Refrigerant	R407C	R410A
Compressor	Fixed-speed scroll	Fixed-speed scroll
Main control	Heating water thermostat	Heating water thermostat
Condenser	Brazed plate	Brazed plate
Evaporator	Fin and coil	Fin and coil
Expansion device	Mechanical TEV	Mechanical TEV
Defrosting method	Reverse cycle	Reverse cycle

[a] Rated according to standard BS EN 14511-2:2004 at an ambient (source) air temperature of 7 °C and a condenser water outlet (heating water supply) temperature of 35 °C.

Details of the two heat pumps are given in Table 1.

Data capture from the two sites consisted of heat meters (optionally reporting individual temperatures and flow rate), current and voltage transducers. A separate measurement of power factor at the laboratory site was found to be 0.924 and no such measurement was made at the field site and so a value of 0.95 was assumed. Data was integrated (or averaged from more frequent sampling as appropriate) and reported at 5-min intervals for the field test site and at 3 s intervals for the laboratory site. (This meant that full defrost transients could be constructed from the latter.) The data set from the field test site was recorded over the main part of one heating season (not the complete heating season) starting in November 2009 and ending in April 2010. For the laboratory site, numerous shorter files of data were obtained and combined.

Checks with instrument manufacturers used at both sites confirmed maximum measurement uncertainties of ± 0.2 K (temperature), ±3% of reading for both current and voltage and ±2% of reading for flow rate. A calculation of equal-odds compound errors with respect to average condenser heat output rates was found to be ±6.6% for the field test installation and ±12.2% for the laboratory installation. For power, average compound errors were found to be ±4.26% (field site) and ±4.22% (laboratory site). The corresponding compound uncertainties with respect to the average *CoP* values were ±7.8% (field site) and ±12.9% (laboratory site). The relatively high compound uncertainty for the heat rate at the laboratory site was due to operating this plant with a relatively high flow rate and low heating temperature differential (usually <4 K) which magnified the impact of the relatively high uncertainties in temperature measurement in the final heat values. Full details of the uncertainty analysis procedure can be found in the Appendix.

Raw results were first processed using the following procedure:

- The data from each site were collected into one file (initially as time-series data) and all random spikes and null reporting rows (i.e. when the heat pump was off) were removed (see Note 1, below)
- All rows containing data during defrost events (evidenced by abnormally low and negative heat rates during phases of steady operation and during low ambient temperatures) were removed (separate files containing these data were retained for later use – see Section 5)
- The data were formed into a matrix of n rows and 4 columns – the first two columns containing the input data (T_{ao}, T_{cwo}) and the other two rows containing the target values (Q_c, W)
- The data were ranked with respect to the T_{ao} values and then averaged using a moving-average resulting in a smaller data set with a reasonable spread (and increment) in T_{ao} values (see Note 2, below)

Note 1:

When the heat pump switches on or off during a logging interval, unrealistic results (mainly power) arise because the variables are evolving from zero within the sampling time interval. Including these results would lead to distortions in the data as far as steady-state heat pump performance is concerned. Therefore these initial switch-on and switch-off time rows of data were discarded.

Note 2:

The purpose of this work was to develop a steady-state heat pump model responsive to variations in boundary conditions but giving results that are essentially static with respect to time. Because the data available from the two data logging systems were essentially dynamic (i.e. logged at either 3 s time intervals in the case of the laboratory heat pump and reported at 5 min intervals in the case of the field trial heat pump) the data were averaged across wider time increments so as to eliminate transient noise such as the response to load disturbances. The sampling interval for averaging was found to have little effect on results for intervals greater than several minutes which suggested that this approach for steady-state modelling was sound. This was confirmed by the quality of results obtained by model-fitting to just one set of data – that of manufacturers' rated performance data which will be evident later.

A multiple objective function optimisation algorithm was used to determine the 10 parameter values of the heat pump model stated formally as follows:

$$\min_{\mathbf{P}} \mathrm{C} \text{ subject to : } \begin{cases} \mathrm{C} \le \mathbf{Goal} \\ \mathrm{P} \ge \mathrm{P}^{-} \\ \mathrm{P} \le \mathrm{P}^{+} \end{cases} \tag{19}$$

The cost function, **C**, was formed from the root-mean-square error values between measured (target) and predicted values of the condenser heat output and heat pump power consumption. The **Goal** vector was set at [0.05 0.1] equivalent to less than 3% of the rated heat and power values of the smaller heat pump (in practice much smaller values were achievable). Initial estimates of the parameter set, **P**, were taken from the average values of the manufacturers' compressor models fitted to data in Fig. 1, from typical values in [19] for the compressor volumetric efficiency model parameters, and deduced from the manufacturers' data on the two heat pumps for the remaining parameters. The lower and upper bound parameter sets, $\mathbf{P}^{-}$ and $\mathbf{P}^{+}$, were initially set at 10% below and above the nominal parameter values respectively. These margins were then increased until solutions were returned within (rather than at) the bounded values. (The Matlab optimization function 'fgoalattain' was used for the above.)

It was found that a very good model could be fitted simply with reference to a single row of inputs and target values. The single row of data for each heat pump was obtained by averaging all of the data in the originally processed set of data. The originally processed set of data was then used as model validation data. Note that the randomness caused by defrost events was dealt with by removing all data rows containing defrost transients so that the model fitting

was carried out using defrost-free data. The data including defrost was however retained for later use (the treatment of defrosting in the heat pump model is dealt with in Section 5).

The averaged model fitting rows of data for the two heat pumps were as follows:

Field data site: $\mathbf{I} = [T_{ao}\ T_{cwo}] = [3.10\ 44.90]$;
$\mathbf{O} = [Q_c\ W] = [4.90\ 2.30]$

Laboratory data site: $\mathbf{I} = [T_{ao}\ T_{cwo}] = [5.93\ 42.38]$;
$\mathbf{O} = [Q_c\ W] = [7.74\ 3.36]$

The fitted model parameters for the two heat pumps are given in Table 2.

Finally, because it was found to be possible to fit an adequate model to a single row of averaged input and target data, it seemed appropriate to consider a similar parameter fitting exercise but this time using the manufacturer's standard rating data (see Table 1). This would then lead to two alternative heat pump models for each site of test data – a 'most optimistic' or 'standard' model based on manufacturer's data and an in-service model based on actual observations.

From Table 1, the standard rating data (according to standard BS EN 14511-2:2004) for the two heat pumps gives the following alternative rows of model-fitting data:

Field data site: $\mathbf{I} = [T_{ao}\ T_{cwo}] = [7\ 35]$;
$\mathbf{O} = [Q_c\ W] = [5.92\ 1.64]$

Laboratory data site: $\mathbf{I} = [T_{ao}\ T_{cwo}] = [7\ 35]$;
$\mathbf{O} = [Q_c\ W] = [10.20\ 2.83]$

Again, the fitted model parameters for the two heat pumps are given in Table 2.

5. Incorporating defrost

The initial model fitting was carried out using average seasonal performance data excluding periods of defrost operation because the latter contains random disturbances in normal heat pump operation and resulted in poor quality model fitting. This requires a model of defrosting to be separately developed and included. A typical energy transient during reverse-cycle defrosting was captured from the laboratory heat pump and is plotted in Fig. 2.

Each defrost cycle lasts typically for about 5 min including periods of inactivity as the changeover valve repositions and a period during which the compressor restarts and the heating delivered drops to a negative value (i.e. heat is sourced from the heating system to effect defrosting in the evaporator).

These defrost events were identified in the original test data sets and two data sets for each heat pump were generated – one including defrost event data and the other in which defrost event data were stripped out prior to averaging. Initial model fitting was carried out using the latter whilst the former were retained for final model testing. Fig. 3 shows the final data sets with and without defrosting. As implied by Fig. 2, Fig. 3 shows that defrosting results in a significant fall in the average heat delivered by the heat pump with only a very small fall in average power consumption. Also, these changes take effect at ambient air temperature below approximately 7 °C. Note that these findings are similar to those reported in [14].

Therefore a simple and sufficient model of defrosting may be envisaged by discounting the average heat output from the heat pump at low ambient temperatures whilst leaving the average power consumption unchanged. A defrost discount factor, F_{df}, is proposed in this work which is defined as the average heat delivered including periods of defrosting divided by the average heat delivered without. Results of this from both measured data sets were found to be very similar and were therefore combined. They are plotted in Fig. 4. The compound uncertainty in F_{df} assuming average heat with and without defrost to be uncertain with equal odds was estimated to be ±15.6%. The defrost discount factor is noted to fall reasonably sharply as ambient temperature fall below approximately 7 °C and then levels off at temperatures below approximately 0 °C. A simple model through the data therefore comprises a linear region and a constant region. In this simple model, the impact of wet bulb temperature on defrost intensity and frequency has not been considered. Indeed Kinab et al. [14] reviewed two similar defrosting models one of which is based on ambient dry bulb temperature and the other on ambient wet bulb temperature. They concluded that the two provided similar results regarding average corrections to heating capacity during low ambient temperatures when defrosting would occur. This seems reasonable since, at the low temperatures involved, winter air states tend to be close to saturation at most times and this means that dry bulb or wet bulb temperature may therefore be used alternatively to some extent. In common with the work reported here, Kinab et al. [14] adopted the model based on ambient dry bulb temperature which, whilst applied to *CoP* rather than Q_c (as in the present work), indicates results that are broadly in agreement with those reported here.

The proposed model is included in Fig. 4.

The model of defrost is applied by adjusting Eqs. (13), (14), (15) as follows:

$$Q_{c,df} = F_{df} Q_c \tag{20}$$

$$CoP = \frac{Q_{c,df}}{W} \tag{21}$$

$$SCoP = \int_{Season} Q_{c,df} \div \int_{Season} W \tag{22}$$

6. Model testing and evaluation

The two models with parameters listed in Table 2 have been tested using the original test data including defrost operating data. Also, included for comparison, are the results of 'most optimistic' models of each heat pump using the parameters derived from the manufacturer's standard rating data for each heat pump (also listed in Table 2). The results are given in Figs. 5–7. Results are plotted against two alternative independent variables – the external air temperature and the overall plant temperature lift (i.e. the difference between the heating water supply temperature and the source air temperature).

Fig. 5 shows results of the two models compared with test data for heat output (Q_c, kW). The models fitted to test data predict the observed data very well in the case of the laboratory heat pump and very well at lower external air temperatures (higher temperature lift) but not so well at higher external air temperatures (lower temperature lift) for the field installation heat pump. However, in the latter case there are insufficient data points in these regions to be conclusive. The average root-mean-square error is 0.30 kW (field heat pump) and 0.58 kW (laboratory heat pump) which is less than 8% of the mean observed heat output of both heat pumps. In both cases, the manufacturer's rated model predicts that slightly higher heat outputs should be obtained from the field heat pump and significantly higher heat outputs from the laboratory heat pump.

Fig. 6 gives results for power consumed (W, kW). The manufacturers' rated models predict power much closer to the models fitted using observed data. Again the laboratory heat pump results agree generally well but the field heat pump models are tending to underpredict power at high ambient temperatures (low temperature lift) though, again, there are insufficient data points in this region. It is most likely that any divergence here is due to the heat pump operating at persistent light load – the transient effects of this are not included in the present model structure which forms an avenue of further work. For power, the average RMS errors between the

Table 2
Fitted parameter results for the heat pump models.

Case[a]	a	b	c	d	E	f	W_{aux}	V_d	ΔT_c	ΔT_e
F-test	0.739	0.179	1.655	8.400	1.090	0.047	0.359	0.0012	5.018	5.054
F-mnf	0.771	0.149	1.703	8.400	1.095	0.040	0.300	0.0013	5.019	5.008
L-test	0.660	0.177	1.153	8.400	0.915	0.040	0.359	0.0014	5.087	4.709
L-mnf	0.737	0.148	1.346	8.400	1.099	0.040	0.272	0.0015	4.905	4.570

[a] F-test = field test data; F-mnf = manufacturer's rated test data (field test heat pump); L-test = laboratory test data; L-mnf = manufacturer's rated test data (laboratory heat pump).

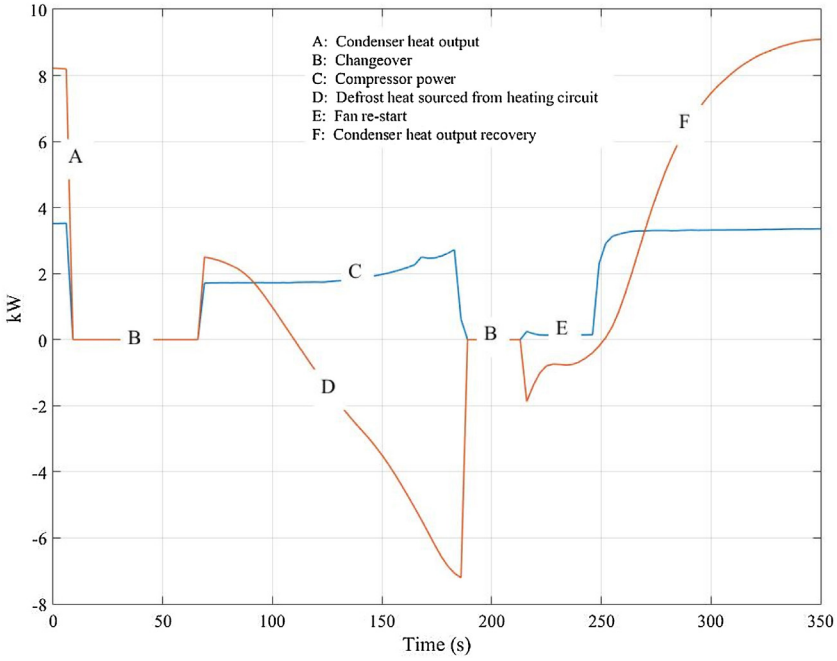

Fig. 2. Transient energy transfers during defrosting (laboratory heat pump).

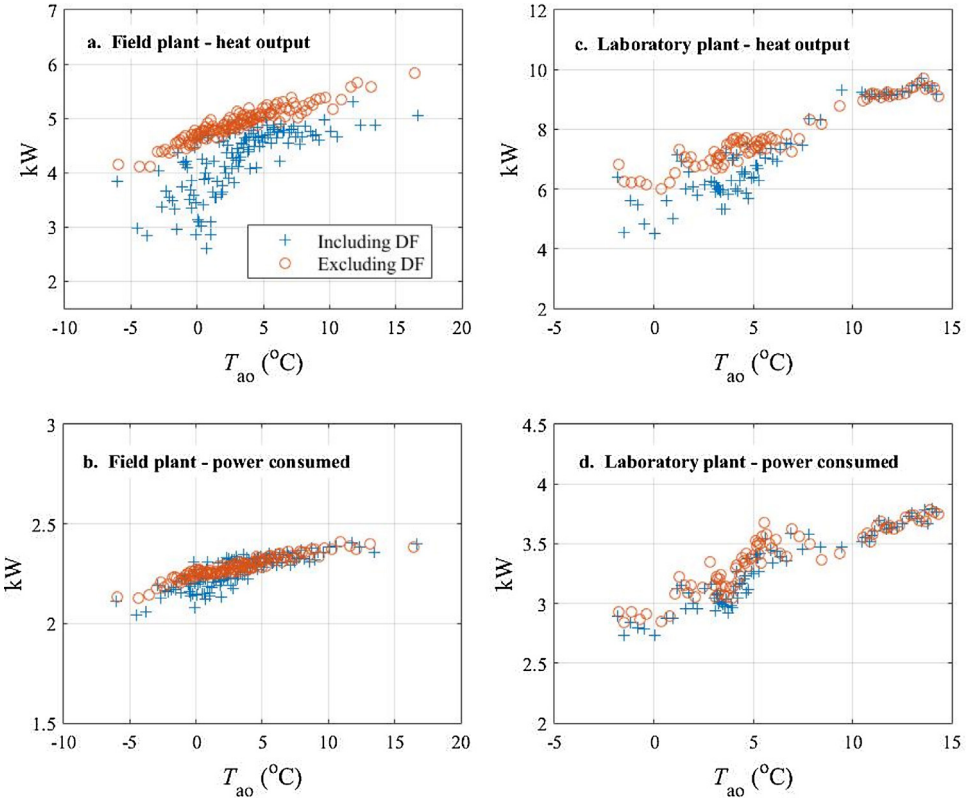

Fig. 3. Heat output and power consumption with and without defrost event data.

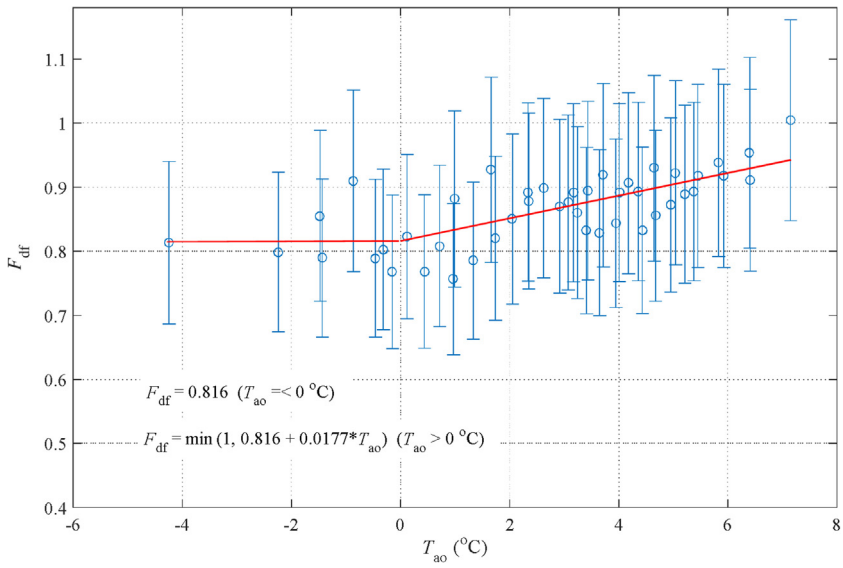

Fig. 4. Proposed defrost discounting model fitted to measured data.

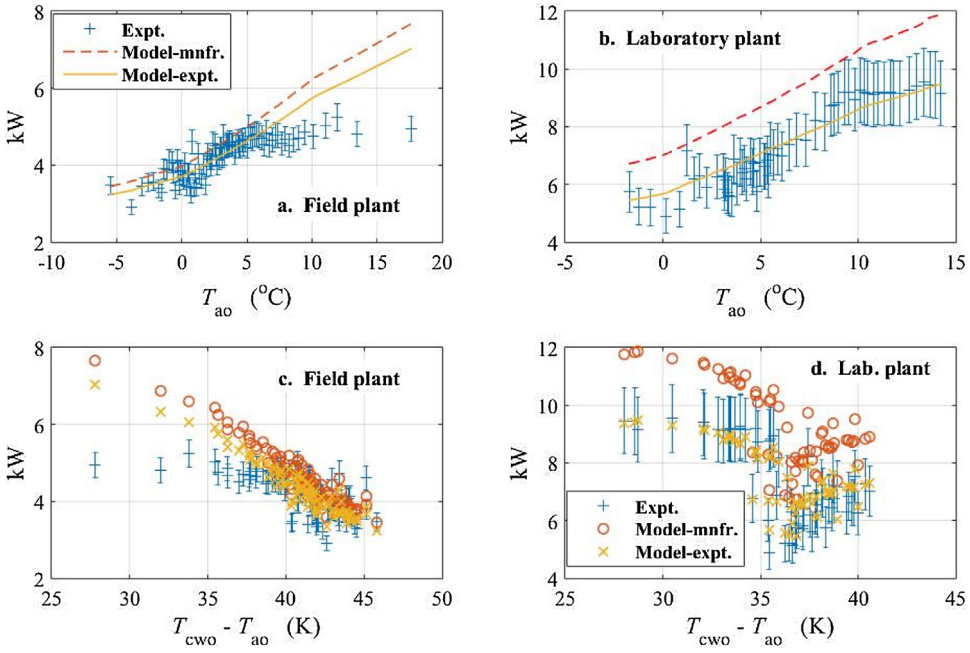

Fig. 5. Model predictions compared with test data – heat output.

models fitted using average observed data and the observed data including defrost is 0.063 kW (field heat pump) and 0.27 kW (laboratory heat pump) – equivalent to approximately 3% and 8% of mean observed values respectively.

Fig. 7 shows the coefficient of performance predictions and observations. Again both models perform best at low external temperatures (high temperature lift) though there are limited data points where the models appear to perform less well. In all cases, models fitted to manufacturers' standard ratings suggest that higher performances (but not dramatically higher) should have been expected from these heat pumps.

Fig. 8 shows the isentropic efficiencies of both heat pump compressors plotted against temperature lift. Using Eq. (6) and Eq. (1) together with the parameters of Table 2, it is possible to deduce the peak isentropic efficiencies based on the experimentally-fitted compressor modelling parameters. These are 0.67 for the field heat pump and 0.60 for the laboratory heat pump. However these results occur at low compression ratios at which the low heating temperature values are likely to be impractical. Nonetheless, Fig. 8 confirms that both compressors are always operating at compression ratios higher than those corresponding to the peak efficiencies as shown in the typical compressor performance curves of Fig. 1. This is an area that requires to be addressed in order to get the very best out of these small plants.

7. Application and verification

In UK practice air-source heat pumps are usually assessed in conjunction with the government's 'standard assessment procedure' – SAP [22]. This can be determined from results generated using the reference simulation model 'BREDEM' [23]. Currently, BREDEM uses a constant effective mean *SCoP* value for domestic

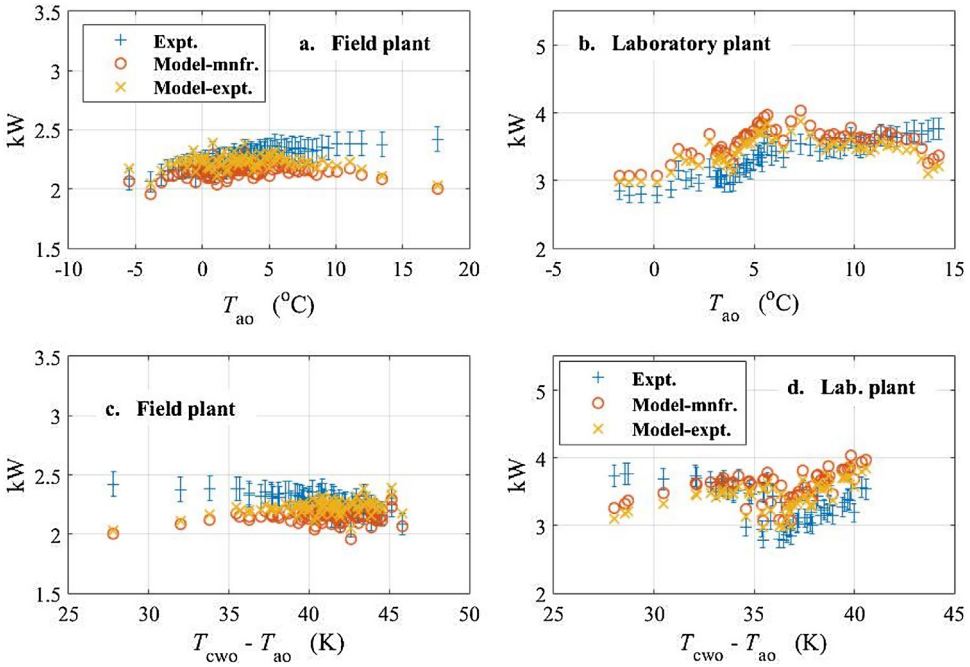

Fig. 6. Model predictions compared with test data – power.

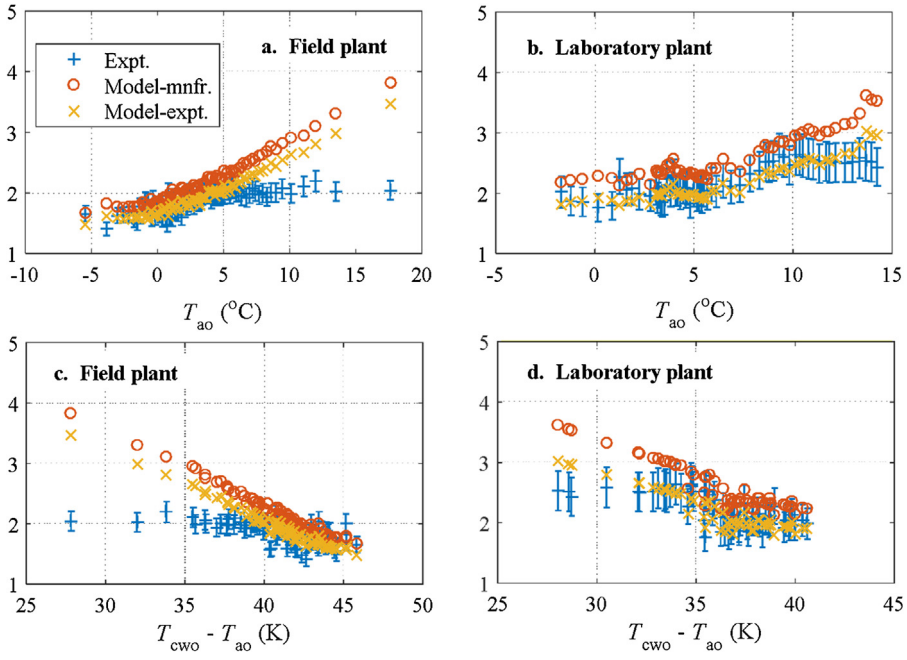

Fig. 7. Model predictions compared with test data – *CoP*.

air-source heat pumps of 2.5. In fact, this has been verified by recent UK field trials of domestic air-source (and other) heat pumps with average results of 2.45 [2] and 2.56 [3]. As a final analysis, the two fitted heat pump models in the present work were applied to a range of heating system operating temperatures and to the monthly average external air temperatures for the 'Thames' region used in BREDEM-12 [23]. The monthly results were then further averaged to form annual *SCoP* values for both heat pumps combined. Results plotted against heating system temperature are shown in Fig. 9. The 'most optimistic' results here are those based on models fitted to manufacturers' standard rating data whereas the 'typical' results are those based on models fitted to the test data used in the present work. The results confirm the recent UK field trial averages for heating system temperatures up to 45 °C [2,3] and also reveal a moderate performance gap with respect to typical values given in manufacturers' technical literature. To achieve the much higher *SCoP* values of 3 or more (for example, reported in [4] based on field trials in other European countries) will require consistently lower heating system operating temperatures then we are accustomed to using in the UK.

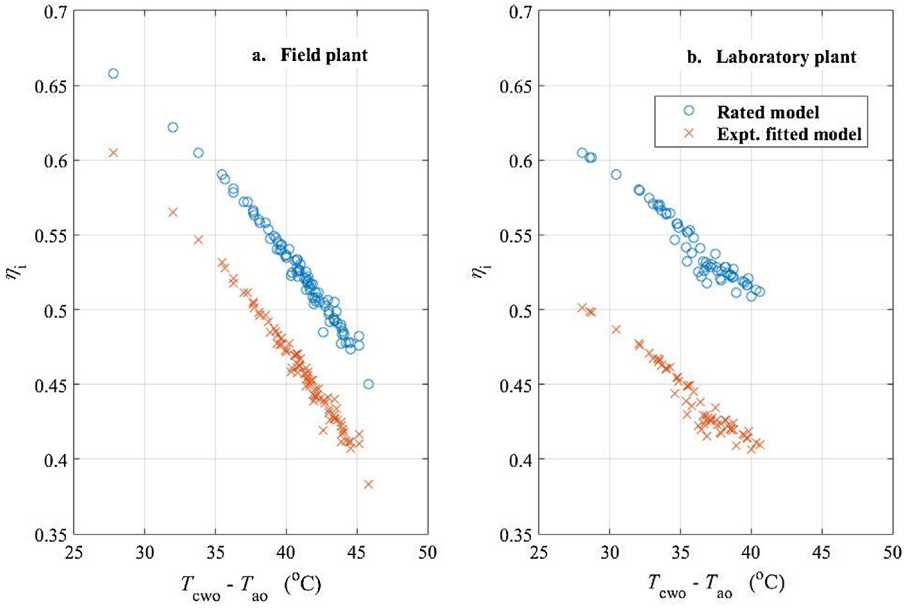

Fig. 8. Compressor isentropic efficiency.

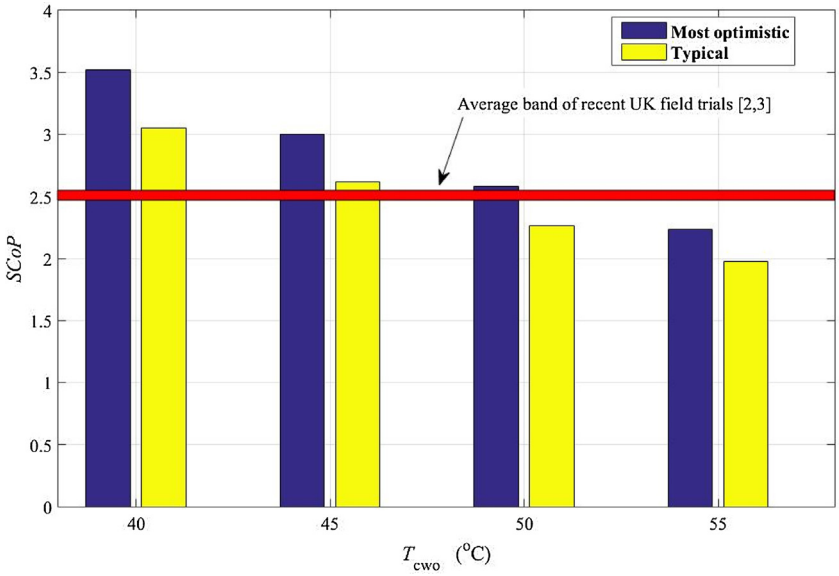

Fig. 9. Overall results compared with alternative field data.

8. Conclusions

A new domestic air-source heat pump model has been reported in this work. The model can be parameterised from either field data or manufacturer's standard rating data and differs from most other regression-type heat pump models in that key heat pump performance parameters such as compressor isentropic efficiency and heat exchange pinch are deduced which enables comparisons between alternative systems to be made.

The model can be parameterised from a small amount of data – mean source air temperature, mean heating system temperature and refrigerant type as inputs; corresponding mean heat output and power consumption as target data. Thus it is possible to parameterise the model from either average seasonal field trial results or from standard rating data with the advantage that it is possible to consider both typical (field data) and most optimistic (rating data) performance scenarios from which considerations into building 'performance gap' might be made.

The model includes a new type of fitted compressor model which leads directly to the compressor isentropic efficiency. Results presented here confirm the relatively low efficiency at which these small compressors operate at in the field compared with larger commercial plant. A model which includes an allowance for defrosting is incorporated which ensures that it tracks performance at low external air temperatures with good accuracy.

Predictive results of heat output and power consumption by the model give root-mean-square errors over test data that are generally significantly less than 10% of the mean test data values. The model has also been verified to provide results that are in broad agreement with recent field monitoring results from UK domestic installations. The model was noted to be less able to predict performance at higher external air temperatures most likely due to transient part-load performance behaviour at these conditions.

However this is more strongly evident in the case of the field test heat pump than in the case of the laboratory heat pump. Because the model reported here is essentially a steady-state model, it will tend to predict increasing heating capacity as the source temperature (and, hence, suction pressure) increases since a greater refrigerant flow rate will be delivered by the compressor. In practice, the heat pump will tend to operate intermittently in these conditions and this will result in a reduction in performance. Remedies for this include thermal buffering (i.e. heat storage in series with the heat pump) and continuous operation with a variable speed compressor drive. None of these details have been included in the model reported here but they have been reported extensively elsewhere (e.g. [21]). In summary, the model reported here will be most suited to application in which the heat pump capacity is well matched to the heating demand throughout the operating cycle.

The overall advantages of a parametric model of the kind reported here are twofold: It can be fitted to limited data sets; and it can be used to reveal detailed parameters on the refrigerant side of the plant such as compressor efficiency and heat exchange thermal approaches. There are three specific areas in which the reported model has advantages over the more commonly reported boundary variable type model:

a) It may be fitted to manufacturer's rated data according to BS EN 14511:2:2004 to describe optimum performance over the heating season which can then be cross-matched to actual performance of the heat pump in the field in order to help identify potential areas of improvement.
b) It may be used where field monitoring data are available but incomplete. In these circumstances, the model may be used to fill in gaps of missing performance data in order to inform longer term performance issues and running costs (e.g. in relation to Renewable Heat Incentive payments).
c) It can be used to evaluate alternative compressor and heat exchanger performances and characteristics.

Avenues for further work are as follows:

- Design and introduce one or more additional parameters to enable the model to fully describe part load performance (which tends to occur when the heat pump is enjoying higher source temperatures – the effects are, to some extent, cancelling)
- Further testing and evaluation using some of the new field data which is starting to become available (e.g. [3]) and the development of strategies to troubleshoot design and installation flaws at specific sites
- Further analysis of the defrost model to consider the impact of other influencing variables such as ambient humidity
- Extension of the heat pump model to include other system components such as thermal storage and top-up heating
- Development of a variable speed compressor/fan model

Appendix A. Calculation of uncertainties

The measured results from both heat pumps averaged over all data are given in Table A1.

The compound uncertainty in heat output, u_Q, from each heat pump arising from individual

uncertainties in the two temperatures, T_1, T_2, and the mass flow rate, m, can be estimated

from the following:

$$u_Q = \pm\sqrt{\left(u_m \frac{\partial q}{\partial m}\right)^2 + \left(u_{T_1} \frac{\partial q}{\partial T_1}\right)^2 + \left(u_{T_2} \frac{\partial q}{\partial T_2}\right)^2} \quad \text{(A1)}$$

Table A1
Averaged results from tested heat pumps.

Measurement	Average value (field trial)	Average value (lab rig)
Heating mass flow rate	0.222 kgs^{-1}	0.750 kgs^{-1}
Heating flow temperature	44.00 °C	42.54 °C
Heating return temperature	39.50 °C	40.19 °C
Power supply voltage	230 V(ac)	224 V(ac)
Power supply current	10.30 A(ac)	15.97 A(ac)
Power factor	0.950	0.924

From the data in Table A1 for the field trial heat pump:

$$\frac{\partial q}{\partial m} = 18.855 kJkg^{-1}; \frac{\partial q}{\partial T_1} = 0.930 kWK^{-1}; \frac{\partial q}{\partial T_2} = -0.930 kWK^{-1}$$

Applying Eq. (A1) leads to a compound uncertainty of ± 0.276 kW with respect to the mean

heat measurement (± 6.6% of the mean measured value).

The same calculation for the laboratory heat pump gave a result of ± 0.90 kW (± 12.2% of the

mean measured value).

Using a similar approach, compound uncertainties for power were found to be ± 0.096 kW

(field heat pump) and ± 0.14 kW (laboratory heat pump) corresponding to ± 4.26% and ± 4.22%

of the mean measured values respectively.

Compound uncertainties in heat pump *CoP* are estimated using the mean heat and power

uncertainty values calculated above using the following:

$$u_{CoP} = \pm\sqrt{\left(u_Q \frac{\partial CoP}{\partial Q}\right)^2 + \left(u_W \frac{\partial CoP}{\partial W}\right)^2} \quad \text{(A2)}$$

And: $\frac{\partial CoP}{\partial Q} = \frac{\partial}{\partial Q}\left(\frac{Q}{W}\right) = \frac{1}{W}$; $\frac{\partial CoP}{\partial W} = \frac{\partial}{\partial W}\left(\frac{Q}{W}\right) = -\frac{Q}{W^2}$

For the field trial heat pump, the compound uncertainty in *CoP* based on measured mean heat

and power values of 4.186 kW and 2.251 kW respectively will be:

$$u_{CoP} = \pm\sqrt{\left(\frac{0.276}{2.251}\right)^2 + \left(-\frac{0.096 \times 4.186}{2.251^2}\right)^2} = \pm 0.146$$

This is ± 7.8% of the mean measured *CoP* value for this heat pump. The same calculation

using the data for the laboratory heat pump gives a result of ± 0.288 which is ± 12.9% of the

mean measured *CoP*.

References

[1] DECC, The Future of Heating: Meeting the Challenge, 2017, Available online: https://www.gov.uk/government/uploads/system/uploads/attachment_data/file/190149/16_04-DECC-The_Future_of_Heating_Accessible-10.pdf. (Accessed 22 August 2016).
[2] Energy Saving Trust, the Heat Is On: Heat Pump Field Trials Phase 2, 2017, Available online: http://www.energysavingtrust.org.uk/sites/default/files/reports/TheHeatisOnweb(1).pdf. (Accessed 18 August 2016).
[3] Department of Energy and Climate Change, Detailed Analysis of Data from Heat Pumps Installed via the Renewable Heat Premium Payment Scheme, 2017, Available online: https://www.gov.uk/government/publications/detailed-analysis-of-data-from-heat-pumps-installed-via-the-renewable-heat-premium-payment-scheme. (Accessed 18 August 2016).
[4] C.P. Gleeson, R. Lowe, Meta-analysis of European heat pump field trial efficiencies, Energy Build. 66 (2013) 637–647.
[5] Zero Carbon Hub, Performance Gap, 2017, Available online: http://www.zerocarbonhub.org/current-projects/performance-gap. (Accessed 22 August 2016).
[6] C.P. Underwood, Chapter 16—Heat pump modelling, in: S.J. Rees (Ed.), Advances in Ground-source Heat Pump Systems, Woodhead Publishing, Amsterdam, 2016.
[7] R. Gupta, R. Irving, Development and application of a domestic heat pump model for estimating CO_2 emissions reductions from domestic space heating

hot water and potential cooling demand in the future, Energy Build. 60 (2013) 60–74.
[8] G. Murphy, J. Counsell, E. Baster, J. Allison, S. Counsell, Symbolic modelling and predictive assessment of air source heat pumps, Build. Serv. Eng. Res. Technol. 34 (1) (2012) 23–39.
[9] S.A. Tabatabaei, J. Treur, E. Waumans, Comparative evaluation of different computational models for performance of air source heat pumps based on real world data, Proc. International Conference on Environmental and Climate Technologies, CONECT' 15 (2015).
[10] M.F. Touchie, K.D. Pressnail, Testing and simulation of a low-temperature air-source heat pump operating in a thermal buffer zone, Energy Build. 75 (2014) 149–159.
[11] F. Madonna, F. Bazzocchi, Annual performance of reversible air-to-water heat pumps in small residential buildings, Energy Build. 65 (2013) 299–309.
[12] H. Jin, J. Spitler, Parameter estimation based model of water-to-water heat pumps withy scroll compressors and water/glycol solutions, Build. Serv. Eng. Res. Technol. 24 (3) (2003) 203–219.
[13] J.J. Guo, J.Y. Wu, R.Z. Wang, A new approach to energy consumption prediction of domestic heat pump water heater based on grey system theory, Energy Build. 43 (2011) 1273–1279.
[14] E. Kinab, D. Marchio, P. Rivière, A. Zoughaib, Reversible heat pump model for seasonal performance optimization, Energy Build. 42 (2010) 2269–2280.
[15] M. Qu, L. Xia, S. Deng, Y. Jiang, A study of the reverse cycle defrosting performance on a multi-circuit outdoor coil in an air source heat pump –Part I: Experiments, Appl. Energy 91 (2012) 122–129.
[16] M. Qu, P. Dongmei, L. Xia, S. Deng, Y. Jiang, A study of the reverse cycle defrosting performance on a multi-circuit outdoor coil in an air source heat pump –Part II: Modelling analysis, Appl. Energy 91 (2012) 274–280.
[17] J. Ji, G. Pei, T.T. Chow, W. He, A. Zhang, J. Dong, H. Yi, Performance of a multi-functional domestic heat pump, Appl. Energy 80 (2005) 307–326.
[18] N.J. Kelly, J. Cockcroft, Analysis of retrofit air source heat pump performance: results from detailed simulations and comparison to field trial data, Energy Build. 43 (2011) 239–245.
[19] ASHRAE Handbook, HVAC Systems and Equipment, Chapter 38 – Compressors, American Society of Heating, Refrigerating and Air Conditioning Engineers, Atlanta, 2016.
[20] NIST REFPROP, Reference Fluid Thermodynamic and Transport Properties ?Standard Reference Database 23, Version 8, National Institute of Standards and Technology, Gaithersburg, 2007.
[21] C.P. Underwood, Fuzzy multivariable control of domestic heat pumps, Appl. Therm. Eng. 90 (2015) 957–969.
[22] SAP- The Government's Standard Assessment Procedure for Energy Rating of Dwellings, 2012, Available online: https://www.bre.co.uk/filelibrary/SAP/2012/SAP-2012_9-92.pdf. (Accessed 11 July 2016).
[23] BREDEM-A Technical Description of the BRE Domestic Energy Model. Version 1.1, 2012, Available online: https://www.bre.co.uk/filelibrary/SAP/2012/SAP-2012_9-92.pdf. (Accessed 11 July 2016).